RESEARCH ARTICLE

National Science Open
3: 20230027, 2024
https://doi.org/10.1360/nso/20230027

Earth and Environmental Sciences

Special Topic: Climate Change Impacts and Adaptation

Ensemble flood predictions for River Thames under climate change

Yurui Fan*

Department of Civil and Environmental Engineering, Brunel University London, Middlesex UB8 3PH, UK

*Corresponding author (email: yurui.fan@brunel.ac.uk)

Received 14 April 2023; Revised 9 November 2023; Accepted 4 December 2023; Published online 11 January 2024

Abstract: In this study, a Bayesian model averaging (BMA)-based ensemble modeling system is proposed to project future flood occurrences for the River Thames using downscaled high-resolution climate projections from the latest general circulation models (GCMs) in the Coupled Model Intercomparison Project Phase 6 (CMIP6). The BMA-based ensemble modeling system integrates multiple hydrological models into the BMA framework to enhance the accuracy of hydrological forecasting, which has shown good performance in validation with the NSE higher 0.91, KGE approaching 0.80, and correlation coefficient higher than 0.96. Daily projections of precipitation and temperature under all four shared socioeconomic pathways were obtained from three GCM models and were further employed to project future potential evaporation. The BMA-based ensemble modeling system was then used to forecast annual maximum flood rates and associated 3-day maximum flood volumes in the future. Our results show that the three GCM models exhibit considerable differences in terms of future flood projections, but all indicate a general increase in flood occurrence and magnitude under future climate change scenarios. The future daily flood events under different climate scenarios are likely to become more severe, as indicated by higher mean, maximum, and 90th quantile values of the AMAX flood series. Meanwhile, the corresponding 3-day flood volumes show varying patterns in terms of mean and extreme flood volumes under different scenarios, but we would have more chances to experience severe 3-day flood volumes in future. The results of our study can provide important information for flood risk management and adaptation planning in the River Thames basin.

Keywords: flood forecasting, climate change, CMIP6, River Thames

INTRODUCTION

River floods are among the costliest natural disasters, resulting not only in severe direct damages and fatalities, but also in considerably wider and longer-term adverse economic consequences [1]. In an age marked by climate change and heightened human activities, flooding risk resilience is becoming increasingly important around the world, which is pivotal for sustaining economic and population growth. This challenge is particularly evident in the UK, where rising emissions from human activities, coupled with unprecedented changes in weather extremes, have resulted in growing floods and posed great threats to local communities. For instance, in 2012, the UK experienced some of its wettest weather in a century, with widespread flooding affecting over 8000 properties and causing £400 million worth of damage. A succession of storms reaching

southern England in the winter of 2013/2014 caused severe floods and £451 million in insured losses. Moreover, due to climate change and human activities, we are experiencing more frequent extreme weather events, particularly flooding. The Environment Agency (EA) reports that more than 5 million people living close to coasts and rivers may be forced to flee their homes as flooding risks increase. In May 2019, the EA warned that at least £1 billion a year needs to be spent on traditional flood and coastal defences in the face of climate change. All these facts demonstrate the urgent need to develop effective flood prediction tools to establish a robust early warning system in response to climate change and human interference.

Reliable flood predictions are crucial for developing corresponding resilience strategies, particularly under changing environmental conditions. However, numerous challenges exist in flood prediction, with one of the most critical being the quantification of various uncertainties. Flood predictions are inherently uncertain due to the necessary simplification of complex natural processes and the limited availability of observations [2]. Extensive uncertainties exist in various processes of flood prediction, such as understanding the effects of climate change that contribute to nonstationary hydroclimatic conditions, describing the interferences of anthropogenic activities, and modelling the hydrological system [3]. Specifically, nonstationary hydroclimatic conditions resulting from climate change and human activities would intensify challenges on flood forecasting, indicating more changes in the frequency and intensity of extreme events [4]. Hydrological processes are dynamic and greatly influenced by temperature and precipitation. Even small changes in climatic conditions can result in considerable shifts in runoff, evaporation, water storage, and associated flooding risks [5].

The River Thames, with a total catchment area of 12,935.77 km^2, is the second-longest river in the UK and has a long history of flooding dating back to the Anglo-Saxon Chronicle of 1099 [6]. The river changes from being tidal to non-tidal at Teddington lock (Kingston) [7]. Climate change predictions suggest an increase in the magnitude and intensity of rainfall as well as a rise in sea level, which could lead to more frequent floods. Additionally, new developments planned in the Thames flood plain could interfere with the effectiveness of existing mitigation measures [6]. Despite several measures in place to manage flood risk, such as the tidal surge barrier, walls, and embankments, many flood defenses are coming to the end of their design life. Plans are in place to manage tidal flood risk for the next 100 years, but effective flood risk forecasting under climate change is required to implement engineering and managerial measures. There are a number of studies addressing floods in UK as well as River Thames under climate change. For instance, Miller and Hutchins [8] reviewed the evidence concerning the combined impacts of urbanisation and climate on urban flooding and urban water quality in UK. Collet et al. [9] analyzed future hot-spots for hydro-hazards in Great Britain through a probabilistic assessment. Visser-Quinn et al. [10] conducted a spatial-temporal analysis of compound hydro-hazard extremes across UK. Kay et al. [11] investigated the climate change impacts on peak river flows through national-scale hydrological modelling and probabilistic projections from UK Climate Projections 2018 (UKCP18).

Although many studies have addressed future floods in the UK under climate change, most of them have relied on climate projections from the Coupled Model Intercomparison Project (CMIP) phases 3 (CMIP3) (e.g., [8,9]), and 5 (CMIP5) (e.g., [10,11]). Few studies have addressed future flood forecasting in the UK based on the latest climate projections from CMIP6. Additionally, various hydrological models have been proposed to project flood events in the UK under climate change, such as the Grid-to-Grid (G2G) model in Kay et al. [11] and the CERF (Continuous Estimation of River Flows), PDM (Probability Distributed Model),

and CLASSIC (Climate and Land-use Scenario Simulation in Catchments) models in Collet et al. [9]. However, ensemble model average methods may provide better performance in mitigating uncertainties in hydrological model structures and generating more reliable flood projections.

Therefore, this study aims to develop an ensemble flood forecasting system for the River Thames under climate change by coupling multiple hydrological models, the Bayesian model average (BMA) technique, and downscaled high-resolution climate projections from CMIP6. In detail, an ensemble streamflow modelling framework will be proposed through integrating multiple hydrological models (i.e., GR4J, Hymod, IHACRES) into the BMA technique. Such a framework will be demonstrated through historical observations at the River Thames. The downscaled climate data will be adopted to drive the BMA-based model to generate historical and future streamflow rates. The annual maximum flow rates and corresponding 3-day flow volume will be identified to reflect flood events in the studied region. The main contribution of this study is to explore impacts of climate change on future flood occurrences at River Thames based on the BMA-based ensemble forecasting framework and the latest climate projections from CMIP6.

RESULTS ANALYSIS AND DISCUSSION

Model calibration and verification

In this study, the three hydrological models (i.e., Hymod, GR4J, and IHACRES) were calibrated through the SCE-UA method [12] based on the streamflow observations at the Kingston station in the River Thames. The calibration period is from 1930 to 1984 whilst the validation period is from 1985 to 2015. The Nash-Sutcliffe efficiency (NSE) coefficient, Kling-Gupta Efficiency (KGE) proposed by Gupta et al. [13], and correlation coefficient were adopted in this study to evaluate the performances of hydrological models in calibration and validation. The BMA method was then employed to integrate those three models with different weights to generate ensemble hydrological predictions.

Figures 1 and 2 show the comparison between streamflow observations and predictions from BMA and different hydrological models in both calibration and validation periods. The results indicate that the predictions from all hydrological models can generally track the corresponding streamflow fluctuations in both periods. This indicates that all three conceptual models are applicable for streamflow predictions at the River Thames. In comparison, the BMA method would be able to generate better streamflow predictions due to the good performances of the hydrological models. Table 1 presents the performances of individual hydrological models and the BMA method evaluated by NSE, KGE, and correlation coefficients for different modelling methods in calibration and validation periods. The results would suggest consistent conclusions with those obtained from Figures 1 and 2. All hydrological models would have good performance with the NSE values larger than 0.79 in the calibration period (the GR4J model can approach 0.89) and larger than 0.81 in the validation period (the GR4J model is around 0.9). Moreover, by integrating the three hydrological models into the BMA framework, better predictions would be generated with an NSE approaching 0.9 in calibration and larger than 0.91 in validation. This can also be concluded by their correlation coefficients. Additionally, the KGE evaluation also demonstrates that BMA method can generate accurate hydrological predictions, with the KGE approaching 0.80 in the validation period. Consequently, the BMA-based ensemble modelling system can be employed for future flood forecasting under climate change.

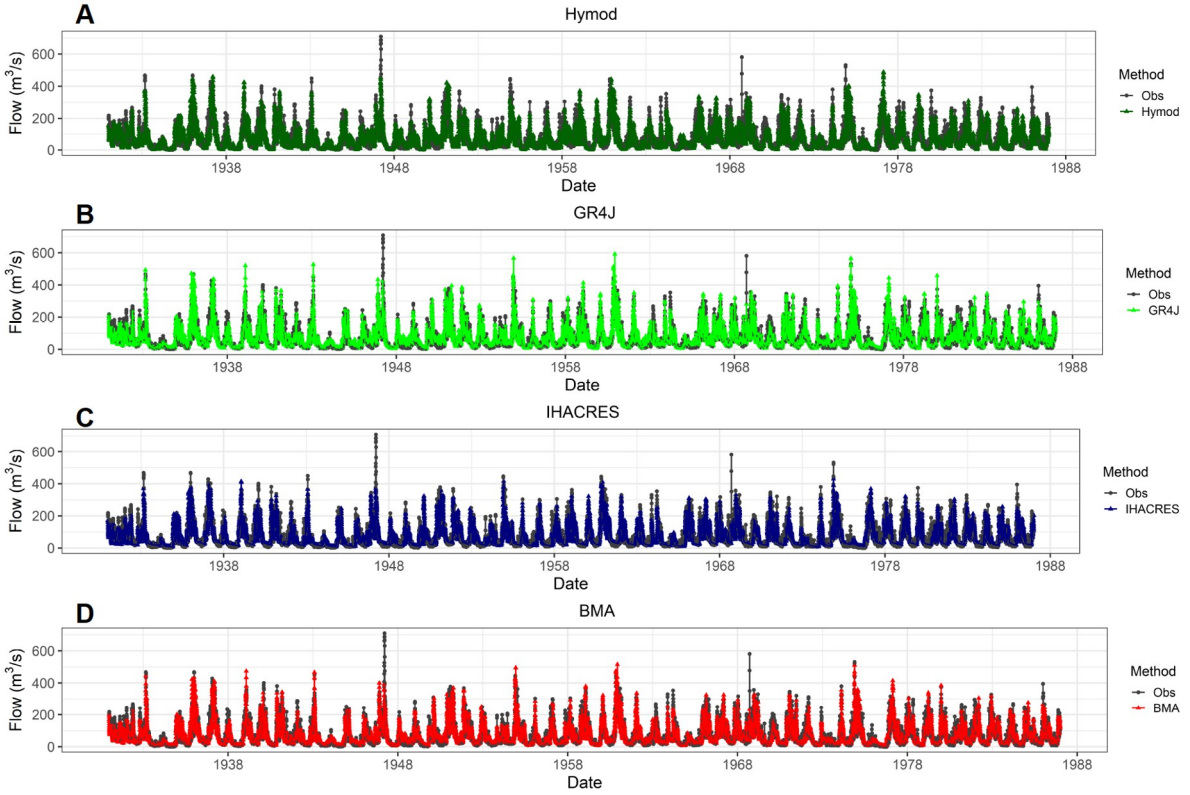

Figure 1 The comparison between observations and predictions from BMA and different models in calibration.

Future climate changes

Future climate changes are one of the major threats for our society. The rising temperature, changing precipitation pattern, and other phenomena are expected to pose significant impacts on natural hazards, especially floods. For the River Thames, significant changes may happen in temperature, precipitation, and the associated potential evapotranspiration, which will further lead to changes in flood occurrence.

Figure 3 presents the changes in daily mean temperature between the historical period (1951–2010) and the future period (2040–2099) based on projections from ACCESS-CM2, ACESS-ESM1-5, and BCC-CSM2-MR under different climate change scenarios. The results suggest apparent temperature increases over the whole River Thames catchment in the future with the highest temperature rise approaching 3.7°C in the southeast part from ACCESS-ESM1-5 under SSP585. However, the spatial patterns of temperature increase would be distinguishable among temperature projections from different GCMs under different SSPs. The northwest part of River Thames catchment would generally have less temperature rises from ACCESS-CM2 and ACCESS-ESM1-5 whilst the southeast part would have larger temperature increases. The outputs from BCC-CSM2-MR indicate a similar temperature change pattern under SSP126. However, under other climate change scenarios, the central or north catchment regions would expect more warming climate. Moreover, outputs from ACCESS-ESM1-5 would indicate more temperature rises around 3.7°C in the southeast under SSP585 whilst BCC-CSM2-MR would project the least temperature increases among the three GCMs with the largest increment around 2.6°C in the north part under SSP585.

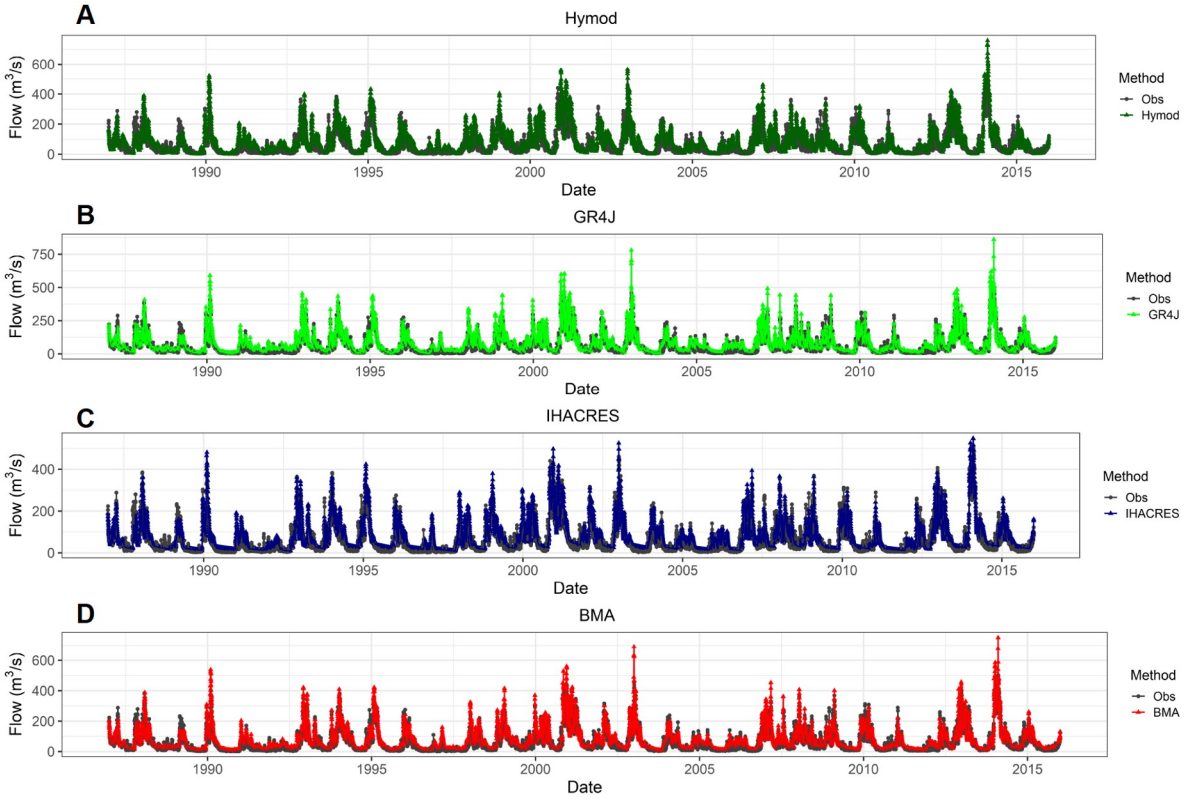

Figure 2 The comparison between observations and predictions from BMA and different models in validation.

Table 1 Efficiency evaluation for different modelling methods

Models	NSE		KGE		Correlation	
	Calibration	Validation	Calibration	Validation	Calibration	Validation
Hymod	0.795	0.816	0.847	0.750	0.905	0.940
GR4J	0.889	0.899	0.868	0.804	0.944	0.959
IHACRES	0.840	0.866	0.844	0.733	0.918	0.947
BMA	0.895	0.912	0.865	0.792	0.947	0.965

Figure 4 presents the changes in annual precipitation between the historical period (1951–2010) and the future period (2040–2099) under different climate change scenarios. The results show noticeable discrepancies among the outputs from different GCMs under different SSPs, suggesting significant uncertainties in future precipitation projections. Under SSP126, both ACCESS-ESM1-5 and BCC-CSM2-MR would project precipitation increments over the River Thames catchment with the largest increment around 34 mm/year in the south part from BCC-CSM2-MR. In comparison, ACCESS-CM2 would project precipitation decreases with the largest decrease around 13 mm/year in the west. However, all three GCMs would project around 20 mm/year rainfall increments under SSP245, but the largest increment may respectively appear in the central south from ACCESS-CM2, southeast from ACCESS-ESM1-5, and west part from BCC-CSM2-MR. Compared with SSP245, less rainfall would happen over the studied area under SSP370 and SSP585 since the rainfall increments would significantly decrease. Some increments would

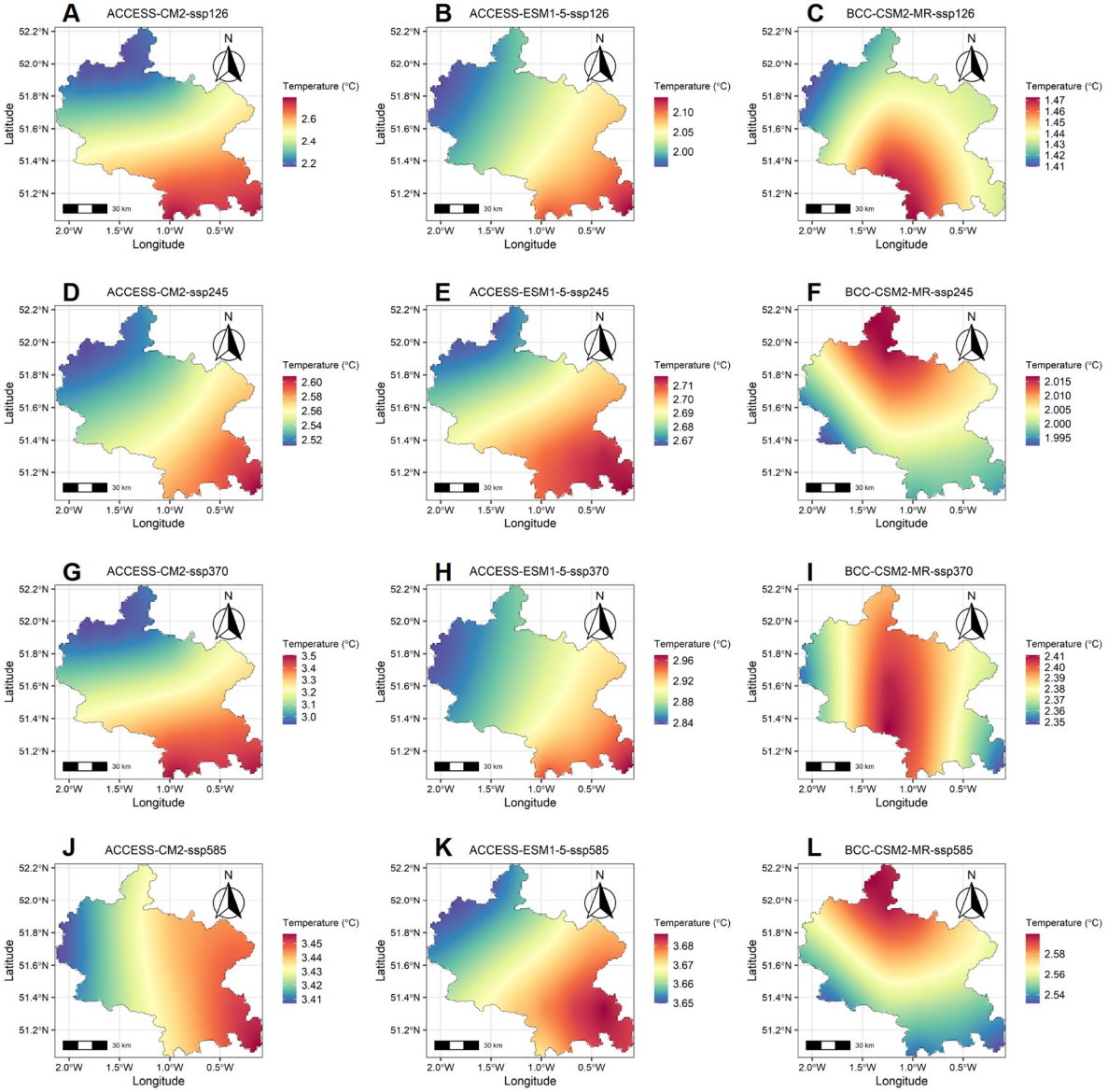

Figure 3 The changes of daily mean temperature between historical period (1951–2010) and future period (2041–2100) from the three GCM models under different climate change scenarios.

become negative, indicating less rainfall when compared with the historical period. Moreover, more rainfall changes may occur in the south or south-east parts from ACCESS-CM2 and ACCESS-ESM1-5 under SSP370 or SSP585 whilst BCC-CSM2-MR would project more rainfall changes in the west part. This also indicates the spatial discrepancies on rainfall changes among the three GCMs.

The changes in temperature and precipitation would also lead to fluctuations for other hydroclimatic variable, such as potential evapotranspiration (i.e., PET). Figure 5 indicates the variations of annual PET between the historical period (1951–2010) and the future period (2040–2099) under different climate change scenarios. Significant increments may occur mainly due to the temperature rises in this region. Moreover, the

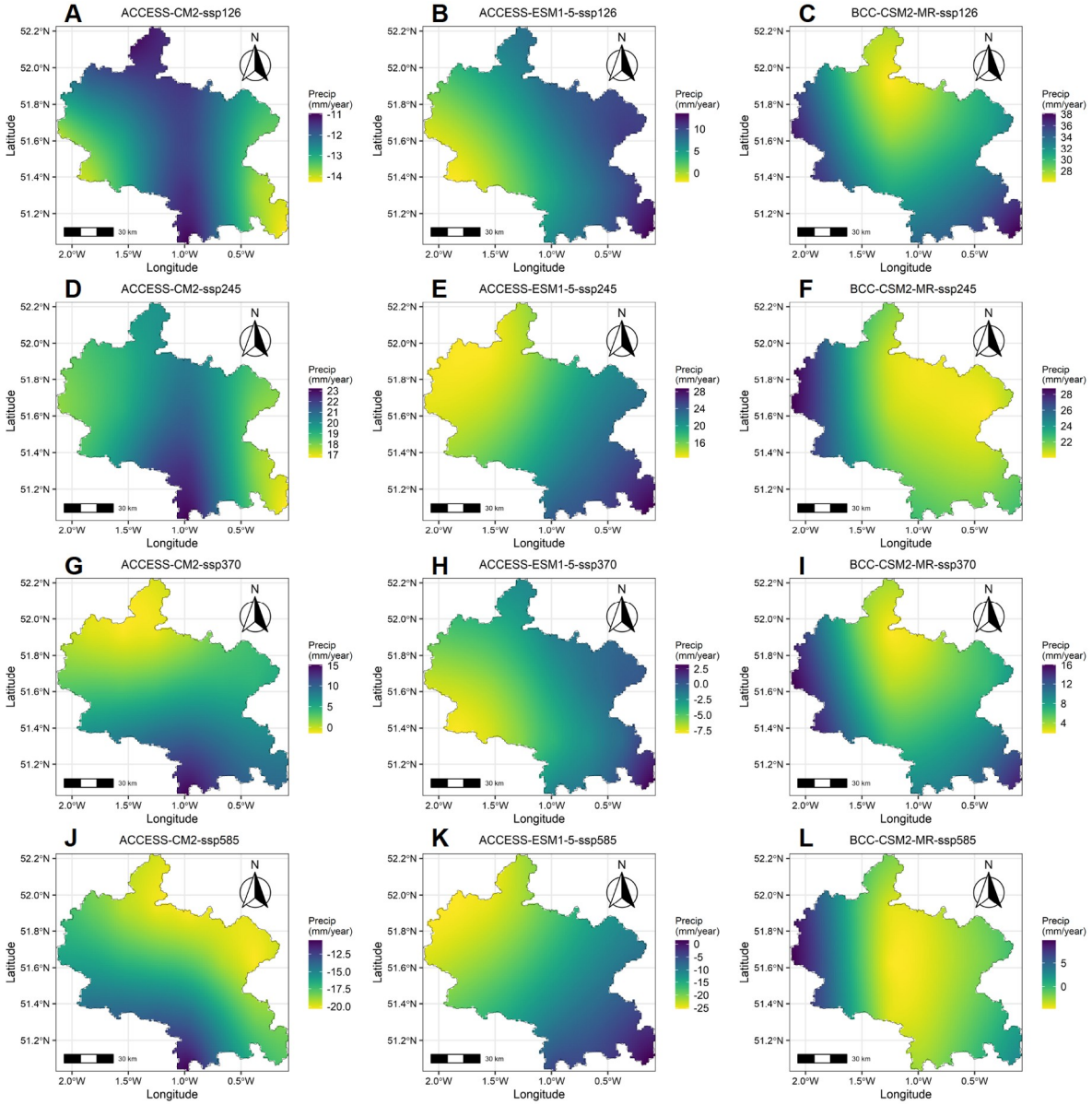

Figure 4 The changes of annual precipitation between historical period (1951–2010) and future period (2041–2100) from the three GCM models under different climate change scenarios.

north or northwest part would have more increases in PET than other regions. Also, the climate projections from ACCESS-ESM1-5 would lead to more PET increases, followed by the projections from ACCESS-CM2 and BCC-CSM2-MR. More PET increments would occur under SSP585 due to the higher temperature rises, with the largest PET increment around 150 mm/year from ACCESS-ESM1-5 in the northwest part.

Future flood projections

As described in the section on future climate changes, many hydroclimatic variables, such as precipitation,

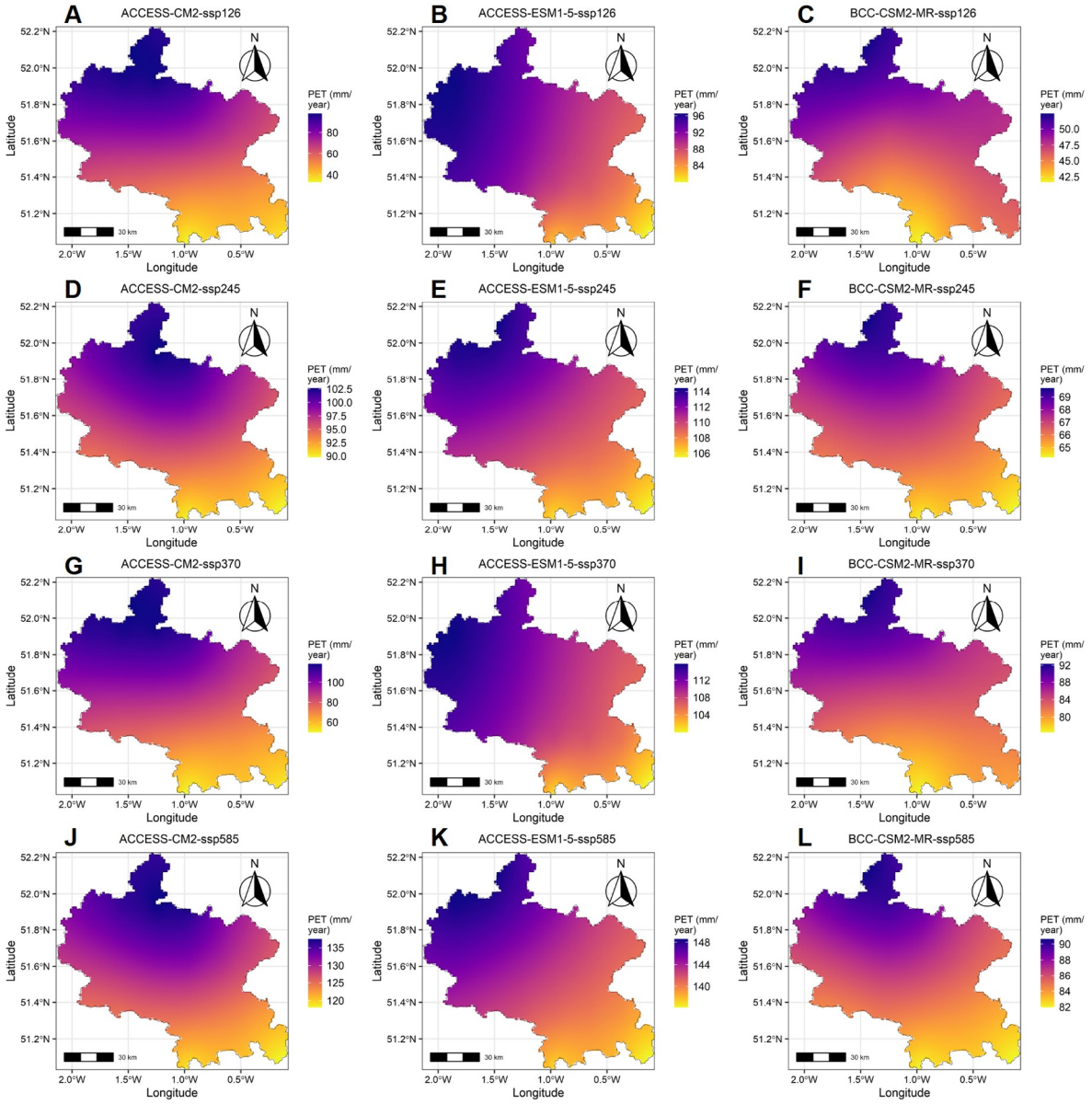

Figure 5 The changes of annual potential evapotranspiration between historical period (1951–2010) and future period (2041–2100) based on climate projections from the three GCM models under different climate change scenarios.

temperature, and PET, are expected to exhibit significant variations in the future due to climate change. These changes will also result in alterations to flood occurrences in the River Thames catchment. Based on the streamflow projections generated by the BMA-based ensemble modeling system, we will characterize the future annual maximum flow rates (AMAX) and associated maximum 3-day flood volumes (referred to as 3-day flood). Also, the historical AMAX and 3-day flood series would be characterized by the historical streamflow simulations.

Based on the climate projections of ACCESS-CM2, Figure 6 displays histograms for the AMAX and 3-day flood series in the historical and future periods. The concentration of both AMAX and 3-day flood series is

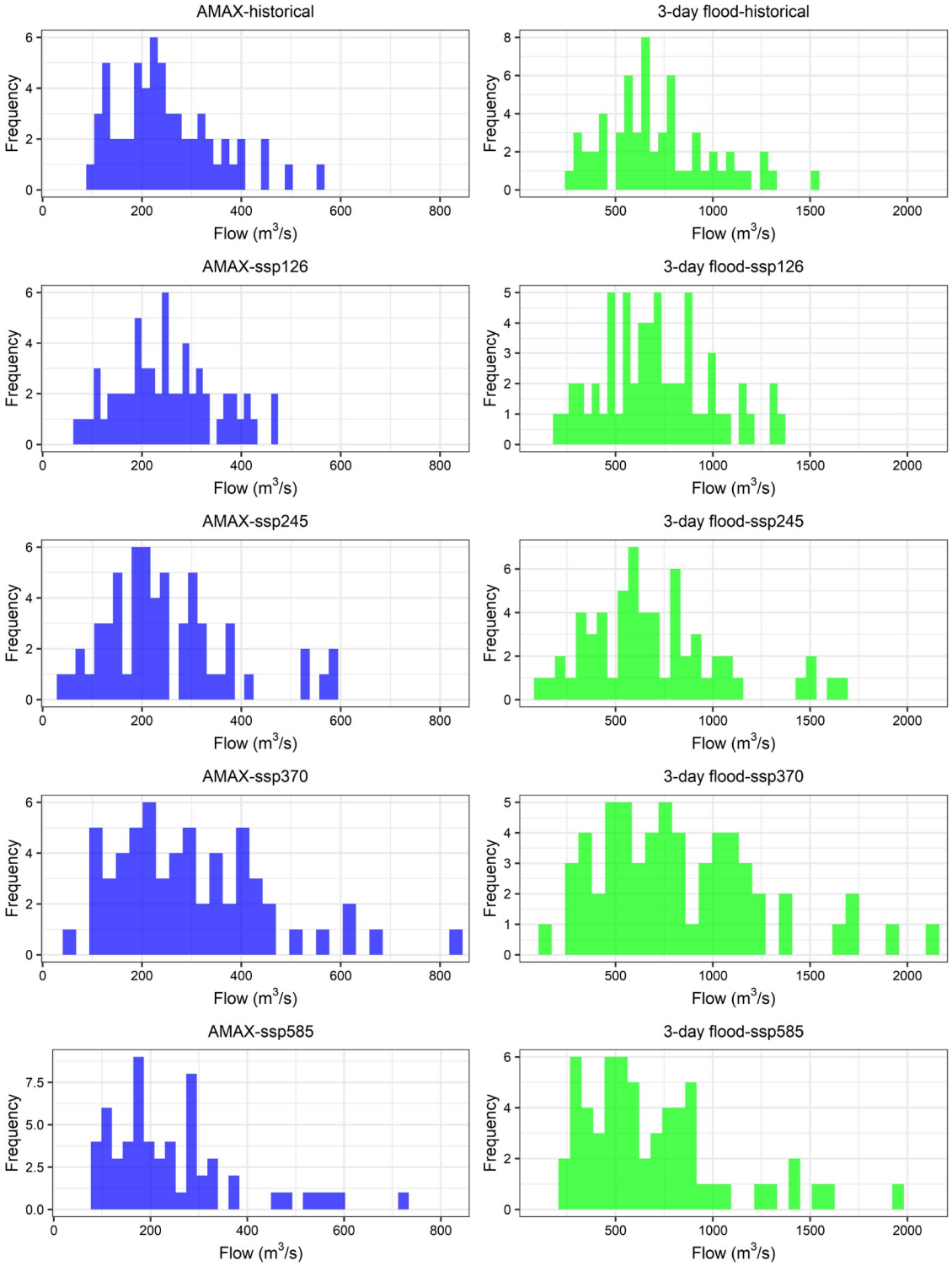

Figure 6 Histograms for AMAX and the associated 3-day flood volumes between historical period and future period driven by climate projections of ACCESS-CM2.

more prominent in the historical period, indicating lower flood variations. However, in the future, flood events demonstrate larger variations, particularly under SSP370 and SSP585. This suggests a greater likelihood of experiencing more significant flood events in the future, despite lower precipitation but higher PET under SSP585 (Figures 4 and 5). Figure 7 displays the histograms of the AMAX and 3-day flood series generated by the BMA-based ensemble modeling system, using climate projections of ACCESS-ESM1-5. These histograms exhibit similar characteristics to those in Figure 6, where the AMAX and 3-day flood series are more tightly distributed in the historical period, whilst future flood events are expected to exhibit greater variability. In addition, the histograms show that even under the relatively mild SSP126 scenario, there is a possibility of experiencing flood events exceeding 800 m^3/s, which suggests a higher risk of severe flooding in the River Thames catchment area under climate change. The histograms in Figure 8 depict the flood projections based on climate projections of BCC-CSM2-MR. Similar to the previous figures, these histograms reveal that more severe flood events may occur in the future. Particularly under SSP245, the maximum flow rate associated with severe flood events may exceed 900 m^3/s, with a corresponding 3-day flood volume larger than 2500 m^3/s. These findings highlight the urgent need for effective flood management strategies to mitigate the potential impacts of climate change on the River Thames catchment.

Table 2 summarizes the annual maximum (AMAX) flood series under different scenarios based on three climate models: ACCESS-CM2, ACCESS-ESM1-5, and BCC-CSM2-MR. The table shows the mean, minimum, maximum, 10th quantile, and 90th quantile values for each model and scenario. For the ACCESS-CM2 model, the mean AMAX values range from 247.3 to 297.7 m^3/s under different scenarios, with no visible increases in mean flood rates except under SSP370. However, higher maximum and 90% quantile values can be observed for the AMAX flood series, particularly under SSP370 and SSP585. For instance, the highest flood rate can reach 820 m^3/s with a 90% quantile of 470 m^3/s, compared to a maximum and 90% quantile flood rate of 559 and 389 m^3/s, respectively. For the ACCESS-ESM1-5 model, the mean AMAX values range from 240.7 to 288.0 m^3/s under different scenarios, showing a clear increase in the future. Although the 90% quantile of the AMAX series does not exhibit significant increases in the future (even decreasing under SSP126), we may observe much higher maximum flood rates, potentially reaching around 800 m^3/s or higher, compared to a maximum flood rate of 453 m^3/s in the historical period. Similarly, for the BCC-CSM2-MR model, the mean AMAX values would show apparent increases in the future, with the highest mean value under SSP245. Moreover, we can also observe significant increments in the 90% quantile values under all climate change scenarios, although the maximum flood rates would not always be larger than that in the historical period. The 90% quantile values would be 375, 420, 443, and 402 m^3/s, respectively, under SSP126, SSP245, SSP370, and SSP585, compared to a 90% quantile value of 324 m^3/s in the historical period. Overall, the table suggests that future flood events under different climate scenarios are likely to become more severe, as indicated by higher mean, maximum, and 90th quantile values of the AMAX flood series.

Table 3 summarizes the 3-day flood volume series based on the climate projections from the three climate models (ACCESS-CM2, ACCESS-ESM1-5, and BCC-CSM2-MR) under different scenarios (historical, ssp126, ssp245, ssp370, and ssp585). For ACCESS-CM2, the mean flood volume ranges from 696.8 to 831.3 m^3/s, with the highest mean value under ssp370 scenario. The minimum flood volume occurs under ssp126, while the maximum and 90% quantile flood volumes are highest under ssp370. For ACCESS-ESM1-5, the mean 3-day flood volume also exhibits an increasing trend as the AMAX flood series in Table 3, with

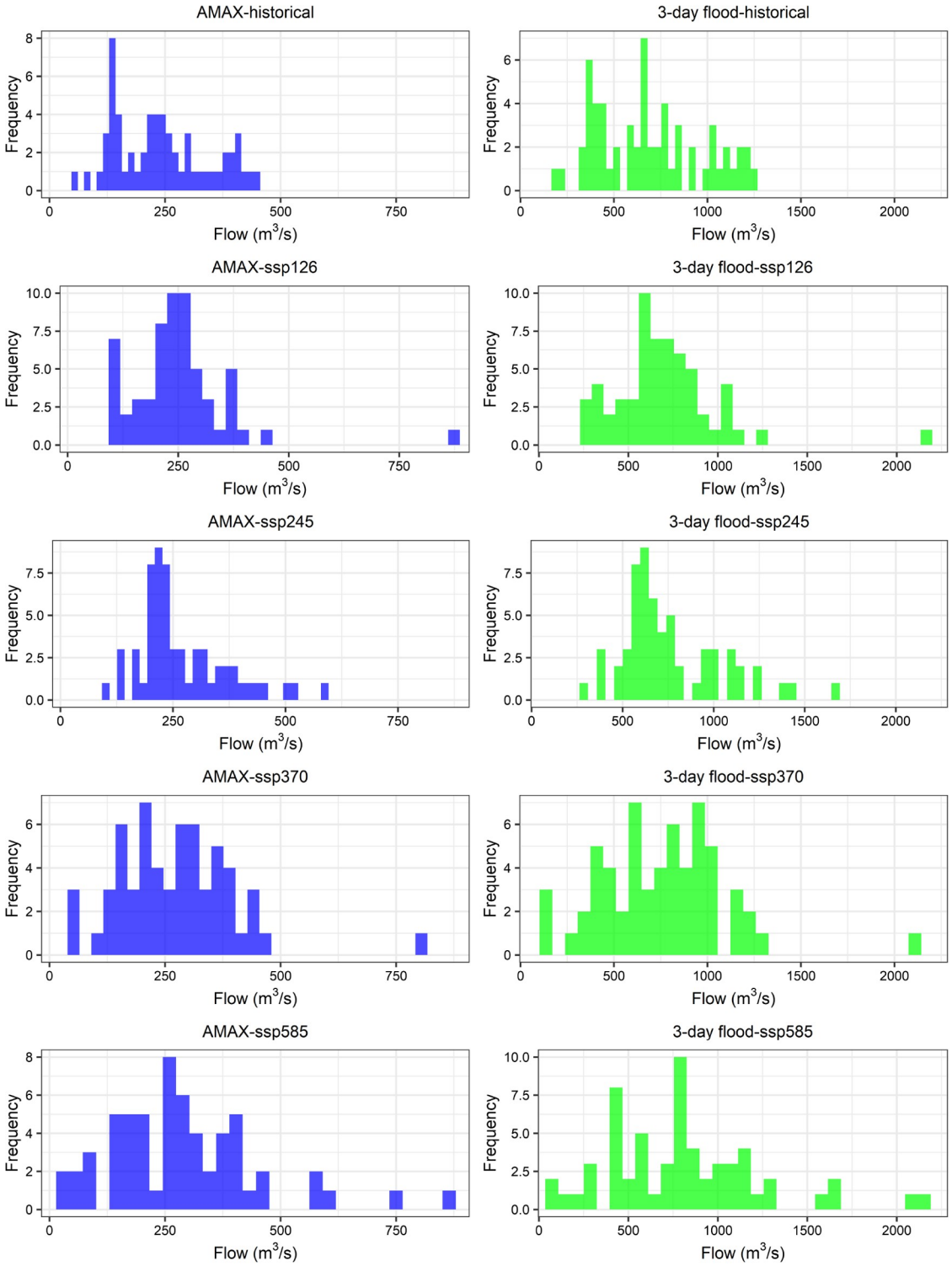

Figure 7 Histograms for AMAX and the associated 3-day flood volumes between historical period and future period driven by climate projections of ACCESS-ESM1-5.

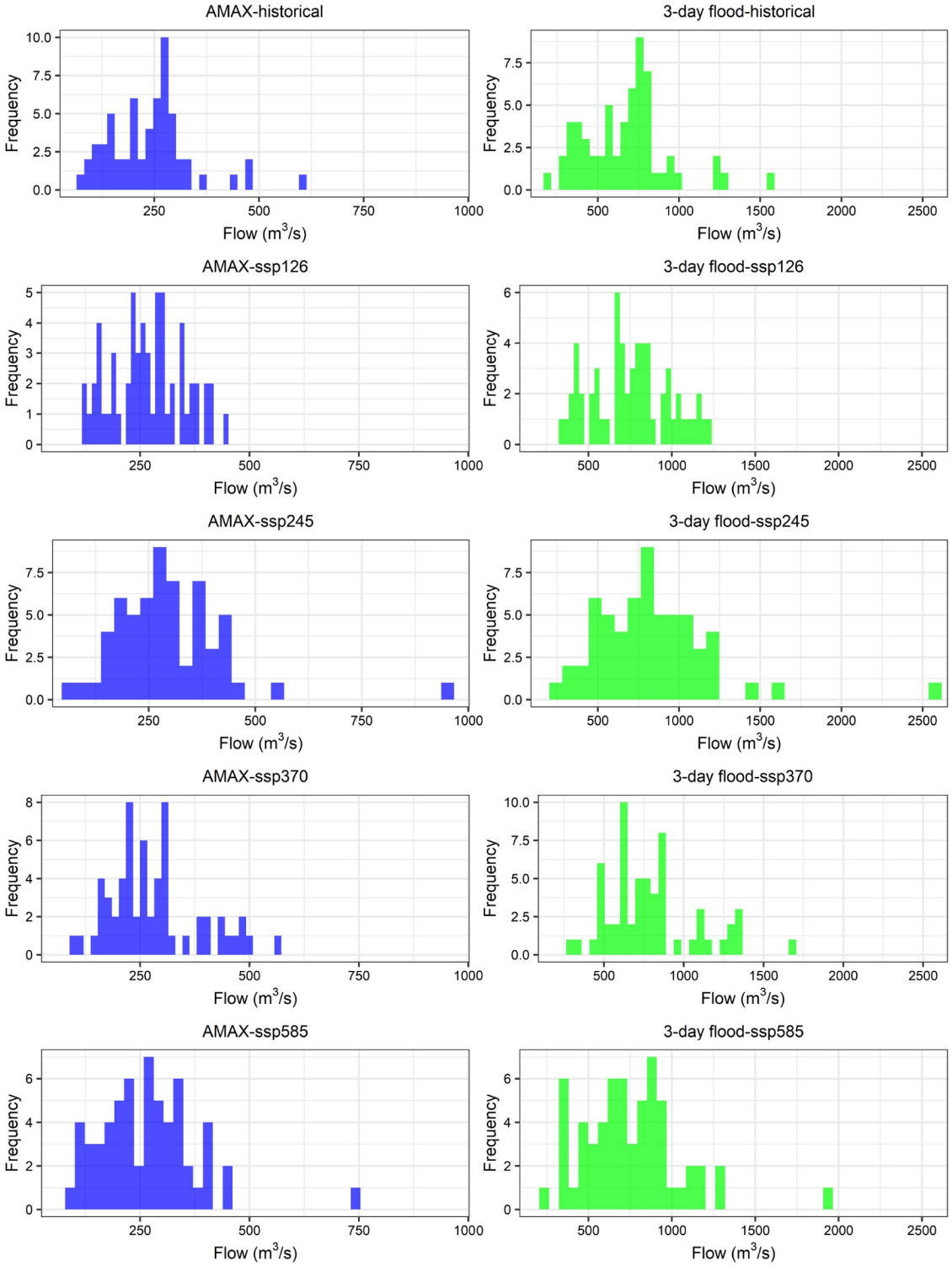

Figure 8 Histograms for AMAX rates and the associated 3-day flood volumes between historical period and future period driven by climate projections of BCC-CSM2-MR.

the highest mean flood values over 804 m^3/s under SSP585. Also, we would observe the largest 3-day flood volume (2180.5 m^3/s) and 90% quantile value (1265.3 m^3/s) under SSP585. As for BCC-CSM2-MR, the mean flood volume ranges from 670.3 to 827.8 m^3/s, with significant increases in the future compared to that in the historical period and the highest mean value under ssp245 scenario. We would also observe higher 90% quantile values and maximum 3-d flood volumes (except SSP126) in the future. Overall, although the three models show varying patterns in terms of mean and extreme flood volumes under different scenarios, we would have more chances to experience severe flood events in the future, as also indicated in Table 3, indicating the urgency for flood resilience in response to future climate changes.

Table 2 Summary for annual maximum (AMAX) flood series

Model	Index	historical	ssp126	ssp245	ssp370	ssp585
ACCESS-CM2	Mean	250.3	250.6	248.3	297.7	247.3
	Min	95.7	71.6	36.1	41.7	85.9
	Max	559.3	469.7	583.6	820.2	721.1
	10Quantile	126.3	125.4	116.3	123.4	106.7
	90Quantile	388.7	388.5	388.5	470.0	467.2
ACCESS-ESM1-5	Mean	240.7	250.9	271.4	272.2	288.0
	Min	58.7	99.1	101.6	45.7	24.0
	Max	453.4	866.8	588.1	798.5	860.3
	10Quantile	129.8	113.5	174.8	138.9	96.9
	90Quantile	401.5	362.5	408.4	400.3	453.0
BCC-CSM2-MR	Mean	240.1	268.4	294.0	281.2	266.5
	Min	70.8	119.2	68.4	96.0	89.1
	Max	602.0	442.9	958.4	563.9	741.4
	10Quantile	121.5	158.7	159.5	167.4	130.1
	90Quantile	324.1	375.2	420.1	443.7	401.8

Table 3 Summary for 3-day flood volume series

Model	Index	Historical	ssp126	ssp245	ssp370	ssp585
ACCESS-CM2	Mean	717.7	709.6	696.8	831.3	689.6
	Min	273.3	200.7	105.4	115.9	236.3
	Max	1536.9	1354.1	1665.1	2107.7	1951.3
	10Quantile	384.6	365.0	328.4	341.2	297.5
	90Quantile	1093.1	1072.7	1080.6	1348.9	1252.5
ACCESS-ESM1-5	Mean	687.6	701.1	760.9	757.4	804.6
	Min	170.3	278.1	296.1	126.1	98.3
	Max	1236.0	2181.5	1679.4	2099.8	2180.5
	10Quantile	368.6	326.7	502.4	392.1	270.8
	90Quantile	1108.2	1034.5	1128.4	1147.5	1265.3
BCC-CSM2-MR	Mean	670.3	757.2	827.8	791.9	747.7
	Min	208.7	339.9	202.7	284.2	250.6
	Max	1583.1	1227.6	2538.2	1677.2	1951.9
	10Quantile	331.4	427.7	462.0	484.6	371.4

CONCLUSIONS

In this study, we proposed a BMA-based ensemble modelling system to forecast future flood occurrences in the River Thames using downscaled high-resolution climate projections from the latest CMIP6 GCM outputs. Our approach integrates multiple hydrological models (i.e., Hymod, GR4J, and IHACRES) into the BMA framework to improve the accuracy of hydrological forecasting. We obtained daily projections of precipitation and temperature for all four shared socioeconomic pathways from three GCM models (ACCESS-CM2, ACCESS-ESM1-5, and BCC-CSM2-MR) and used them to project future potential evaporation. The resulting projections were then used to drive the BMA-based ensemble modelling system, enabling us to forecast annual maximum flood rates and associated 3-day maximum flood volumes in the future.

All the three hydrological models would perform well in the studied area with an NSE value around 0.80 or even higher in calibration and ranging from 0.81 to 0.89 in validation. But the BMA method can further enhance the predictive accuracy for streamflow with an NSE approaching 0.9 in calibration and larger than 0.91 in validation, demonstrating the applicability of the BMA-based ensemble modelling system for future flood forecasting under climate change.

In terms of future climate changes, significant temperature rises would be observed in the River Thames region, with the highest temperature increment around 3.7°C in the southeast part from ACCESS-ESM1-5 under SSP585. However, the future precipitations would show considerable variations compared to those in the historical period. Visible increases in precipitation (around 20 mm/year) may be observed from projections of all three GCMs under SSP245, even though the spatial pattern in rainfall increases would be different among those projections. However, rainfall may also decrease in future from projections of ACCESS-CM2 and ACCESS-ESM1-5 under SSP585, which can approach 20 mm/year in the north or northwest part of the studied area. Due to temperature rises, there would be more potential evapotranspiration in the future, with the highest increment approaching 150 mm/year under SSP585.

The future annual maximum flood rates and the associated 3-day flood volumes are characterized by the streamflow projections based on the BMA-based ensemble modelling system and climate projections from three GCMs. The ACCESS-CM2 model showed the highest potential future flood risk, with the largest increase in flood rates under SSP370. The ACCESS-ESM1-5 model also showed an increase in flood rates in the future, with the highest flood rates projected under SSP585. In contrast, the BCC-CSM2-MR model showed decreases in maximum flood rates under SSP126 and SSP370, but apparent increases in the mean flood rates and 90% quantile values. In general, the results suggest that under different future scenarios, there may be an increase in the frequency and severity of flooding events in the River Thames. The magnitude of these increases varies among the three GCM models and the different socioeconomic pathways. However, the projections consistently suggest that the risk of more frequent and severe flooding in the River Thames should be considered in future planning and management efforts. The findings also highlight the importance of using ensemble modeling approaches that account for model uncertainties and capture a range of potential future outcomes.

There are still some limitations in the current study to be further addressed. Firstly, the climate projections were directly used to drive hydrological models without bias-correction process based on local observations at River Thames. This may lead to a mismatch in retrospective flood occurrence between historical simulations and real observations. Also, outputs from three GCMs were adopted in this study, which may only

show limited uncertainty in future climate projections. More importantly, the results show that projections from different GCMs would lead to varied flood events. Nevertheless, it is still unclear how much contribution the uncertainty in climate projections will make to the future flood risks.

STUDY AREA AND DATA

River Thames

The River Thames, depicted in Figure 9, is the longest river in England, located at a longitude and latitude of 51°35′8.07″N and 0°36′57.87″W, respectively. It stretches 346 km from its source in Gloucestershire towards

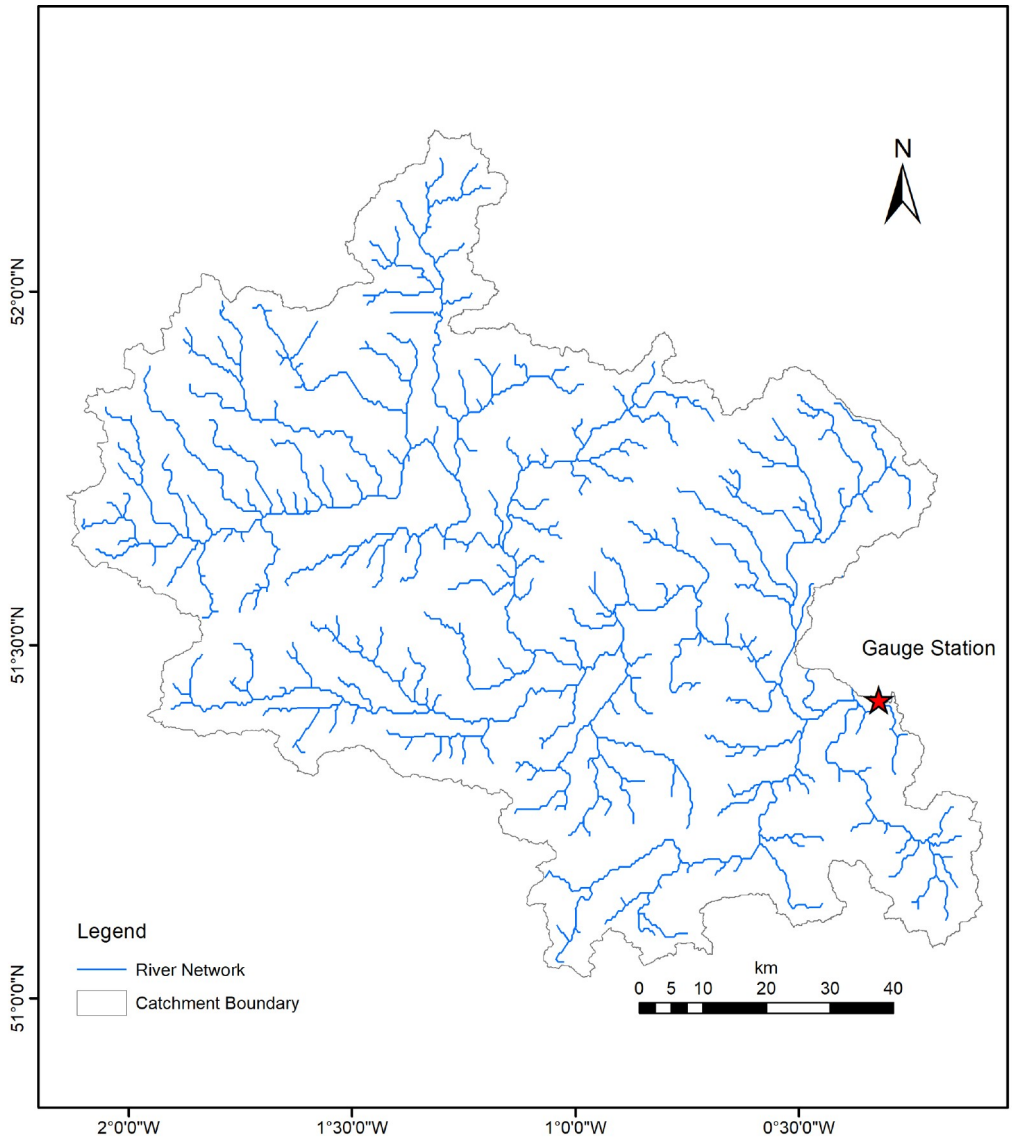

Figure 9 The spatial distribution of the Thames River Basin and associated hydrological gauge station.

the east, emptying into the North Sea, and has a total catchment area of 12,935.77 km^2 [14]. The basin receives an average precipitation of 710 mm, which is evenly distributed throughout the year, except for autumn or early winter when the precipitation peaks. The river basin has a temperate climate with oceanic influence, with summer and winter temperatures of 16.4°C and 4.6°C, respectively, and a mean air temperature of 11°C [15]. The land cover comprises mainly of arable agriculture and pasture throughout the catchment, while forests and urban areas are primarily located at the lower side of it [16]. The lower Thames is facing significant flood risks due to an increase in rainfall, particularly during the winter season [17]. Flooding has been one of the major challenges for the River Thames in the 20th/21st century, with major floods occurring in 1947 and 2007 [18]. The daily streamflow records from 1930 to 2015 at the Gauge station at Kingston are adopted to calibrate and verify the hydrological models. The associated daily precipitation data are also obtained from the National River Flow Archive (https://nrfa.ceh.ac.uk/), and the daily potential evapotranspiration (denoted as PET) data are obtained through averaging the historic gridded potential evapotranspiration developed by Tanguy et al. [19].

Future climate projections

Future climate projections are required to project future flood events for the River Thames under climate change. In detail, high-resolution daily projections with a spatial resolution of 0.25 degree are obtained from the NASA Earth Exchange Global Daily Downscaled Projections CMIP6 (NEX-GDDP-CMIP6) [20]. Three climate models, namely ACCESS-CM2, ACCESS-ESM1-5, and BCC-CSM2-MR, are selected in this study to reflect uncertainties in climate projections. ACCESS-CM2 is one of the two ACCESS global coupled model versions run by the Australian climate community for the Coupled Model intercomparison Project, CMIP, which provides extensive datasets for a number of climate variables such as temperature, rainfall, cloud cover, sea-ice extent, and ocean circulation. ACCESS-ESM1-5 is another GCM model participating in CMIP6 from Australian Community Climate and Earth System Simulator (ACCESS), which includes an interactive carbon cycle [21]. BCC-CSM2-HR is a high-resolution version of the Beijing Climate Center (BCC) Climate System Model, which has been demonstrated to well capture the observed global warming trends from 1950 to 2014 [22].

Four shared socioeconomic pathways (i.e., SSP126, SSP245, SSP370, and SSP585), respectively lower, intermediate, medium-high, and high GHG emission levels, would be considered to characterize the impact of different climate change scenarios on the flood occurrence at the River Thames. For each model, historical simulations during 1951–2010 and future projections during 2041–2100 under all four SSPs for daily precipitation (i.e., pr), maximum air temperature (i.e., tasmax) and minimum air temperature (i.e., tasmin) are obtained from NEX-GDDP-CMIP6. Based on pr, tasmax, and tasmin, the future daily potential evapotranspiration (i.e., PET) would be generated through the Modified-Hargreaves (MH) method [23]:

$$\mathrm{PET} = 0.0025 \times 0.408 \times \mathrm{RA} \times \left(T_{\mathrm{avg}} + 16.8\right) \times \mathrm{TD}^{0.5}, \quad (1)$$

where RA is extraterrestrial radiation expressed in (MJ m^{-2} d^{-1}), T_{avg} is average daily temperature (°C) defined as the average of the mean daily maximum and mean daily minimum temperature, and TD (°C) is the temperature range, computed as the difference between mean daily maximum and mean daily minimum temperature.

METHODOLOGY

Hydrological models

In this study, three different hydrological models will be used, namely Hymod, GR4J, and IHACRES in Figure 10, to forecast future floods for the River Thames under climate change. Hymod (Figure 10A) is a probability-distributed model consisting of three components: a Pareto distribution for reflecting soil storage capacity, a slow-flow tank for routing groundwater flow, and three identical quick-flow tanks for routing surface flow [24,25]. Five parameters (Table 4) need to be calibrated/quantified, and two inputs, precipitation (P (mm/day)) and potential evapotranspiration (PET (mm/day)), are required. State variables in Hymod include the storage in the nonlinear tank representing the watershed soil moisture content, the three quick-flow tank storages representing the temporary (short-time) detentions, and the slow-flow tank storage (subsurface storage) [26].

GR4J (shown in Figure 10B) is a lumped hydrologic model with four parameters (as presented in Table 4), and its structure includes an interception reservoir for intercepting rainfall and PET, a soil moisture accounting procedure for generating effective rainfall, and a water exchange term for modeling water losses to or gains from deep aquifers. The routing module of GR4J consists of two flow components with a constant volumetric split (10%–90%), two unit hydrographs, and a non-linear routing store. More details about GR4J can be found in some literature (e.g., [27–29]).

The IHACRES model [30,31] is another conceptual rainfall-runoff model to be employed in this study. It typically has 5–7 unknown parameters and has many versions developed by a number of studies (e.g., [32–35]). In this study, IHACRES model based on catchment moisture deficit (CMD) [36] will be used. It consists of two modules: (1) a nonlinear module that generates effective rainfall and the CMD output, and (2) a linear module that translates effective rainfall into streamflow by routing it through two parallel linear stores based on the instantaneous unit hydrograph theory [37]. Six unknown parameters, as shown in Table 4, need to be calibrated for the IHACRES model in this study.

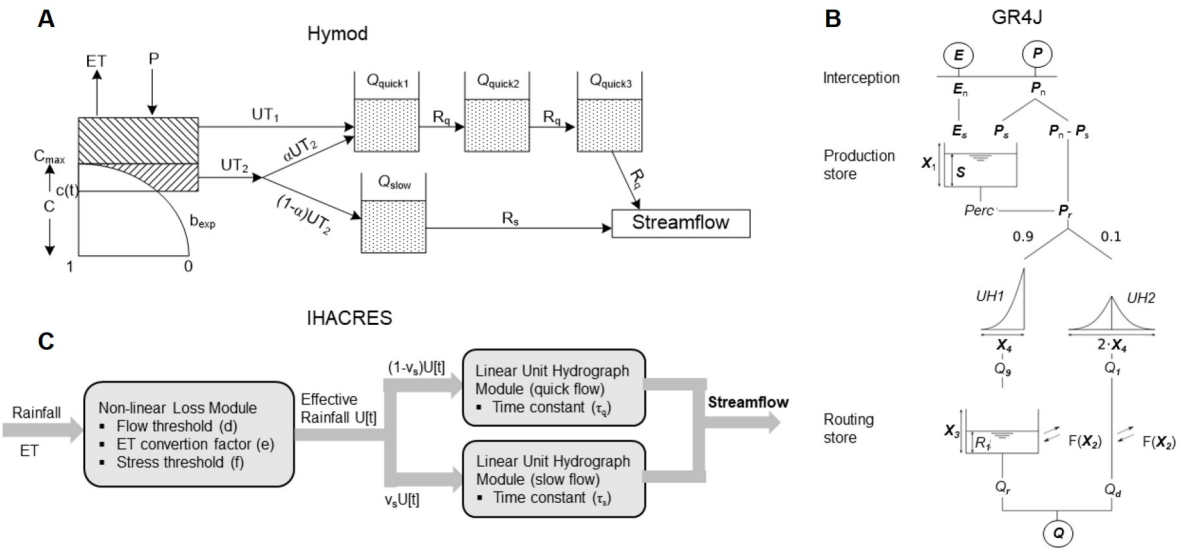

Figure 10 The model structures for Hymod, GR4J, and IHACRES (modified from [38]).

Table 4 Model parameters for Hymod, GR4J, and IHACRES

Models	Parameters	Description	Range
Hymod	C_{max} (mm)	Maximum storage capacity of watershed	[200, 700]
	b_{exp}	Spatial variability of soil moisture capacity	[05, 65]
	α	Factor distributing flow to the quick-flow tank	[01, 09]
	R_s (1/day)	Residence time of the slow-flow tank	[0001, 02]
	R_q (1/day)	Residence time of the quick-flow tank	[01, 09]
GR4J	X_1 (mm)	Capacity of the production soil (SMA) store	[100, 1200]
	X_2 (mm)	Groundwater exchange coefficient	[−5, 3]
	X_3 (mm)	Capacity of the routing store	[20, 300]
	X_4 (day)	Time parameter for unit hydrographs	[05, 4]
IHACRES	τ_q (day)	Time constant governing the rate of recession of quickflow	[05, 10]
	τ_s (day)	Time constant governing rate of recession of slowflow, $\tau_q < \tau_s$	[10, 350]
	V_s	The proportion of slow flow to total flow	[0, 1]
	d (mm)	CMD threshold for producing flow	[50, 550]
	e	Conversion parameter from potential evapotranspiration to actual evapotranspiration	[001, 15]
	f	CMD stress threshold as a proportion of d	[001, 3]

Bayesian model average

Extensive uncertainties would challenge flood projections under climate change, in which the structural uncertainty in hydrological models is one of the most important uncertainties to be considered [39]. The BMA method is adopted in this study to enhance the accuracy for flood projections under climate change. It is a popular ensemble method of multiple models and can successfully integrate the merits of the multitude of candidate models and reduce the predictive uncertainty caused by a single model [40–45].

Let y denotes the forecasted variable, $D_{obs} = \{y_1, y_2, \ldots, y_T\}$ denotes the real observations during the model calibration period. Suppose that there are k alterative hydrological models (denoted as f_i, i =1, 2, …, k) to be used for hydrological predictions. However, it is unknown which model is best, leading to uncertainties in choosing hydrological models. Based on the given observations, D_{obs}, the probability density function (PDF), $p(y|f_1, f_2, \ldots, f_k, D_{obs})$, can be expressed as

$$p(y \mid f_1, ..., f_k, D_{obs}) = \sum_{i=1}^{k} p(f_i \mid D_{obs}) p_i(y \mid f_i, D_{obs}), \tag{2}$$

where $p_i(y \mid f_i, D_{obs})$ is the posterior distribution of y based on model f_i alone. $p(f_i \mid D_{obs})$ denotes the posterior probability of statistical model f_i, known as the likelihood of model f_i being the correct prediction given D_{obs}. It can reflect how well model M_i matches the observations. Since the sum of posterior model probabilities is equal to one (i.e., $\sum_{i=1}^{k} p(f_i \mid D_{obs}) = 1$), they can be considered as weights of the candidate models and Equation (2) can be reformulated as

$$p(y \mid f_1, f_2, ..., f_k) = \sum_{i=1}^{k} w_i p_i(y \mid f_i, D_{obs}), \tag{3}$$

where $w_i = p(f_i \mid D_{obs})$. The posterior mean and variance of the BMA prediction can be expressed as [46]

$$E(y \mid D_{\text{obs}}) = \sum_{i=1}^{k} w_i f_i, \tag{4}$$

$$Var(y \mid D_{\text{obs}}) = \sum_{i=1}^{k} w_i \left(f_i - \sum_{i=1}^{k} w_i f_i \right) + \sum_{i=1}^{k} w_i \sigma_i^2, \tag{5}$$

where σ_i^2 is the variance associated with model prediction f_i with respect to observation D_{obs}. Many methods have been developed to estimate the parameter w_i and σ_i in Equations (4) and (5). In this study, the expectation-maximization (EM) algorithm will be used which is recommended by Raftery et al. [42].

Funding

This work was supported by the Royal Society International Exchanges Program (IES\R2\202075).

Author contributions

Y.F. designed the research, collected research data, performed calculations and results analysis and drafted the paper.

Conflict of interest

The author declares no conflict of interest.

References

1 Dottori F, Szewczyk W, Ciscar JC, *et al.* Increased human and economic losses from river flooding with anthropogenic warming. *Nat Clim Change* 2018; **8**: 781–786.
2 Götzinger J, Bárdossy A. Generic error model for calibration and uncertainty estimation of hydrological models. *Water Resour Res* 2008; **44**: W00B07.
3 Renard B, Kavetski D, Leblois E, *et al.* Toward a reliable decomposition of predictive uncertainty in hydrological modeling: Characterizing rainfall errors using conditional simulation. *Water Resour Res* 2011; **47**: W11516.
4 Fan YR, Yu L, Shi X, *et al.* Tracing uncertainty contributors in the multi-hazard risk analysis for compound extremes. *Earths Future* 2021; **9**: e2021EF002280.
5 Hirabayashi Y, Mahendran R, Koirala S, *et al.* Global flood risk under climate change. *Nat Clim Change* 2013; **3**: 816–821.
6 Lavery S, Donovan B. Flood risk management in the Thames Estuary looking ahead 100 years. *Phil Trans R Soc A* 2005; **363**: 1455–1474.
7 Sanders R, Tabuchi S. Decision support system for flood risk analysis for the River Thames, United Kingdom. *Photogramm Eng Remote Sens* 2000; **66**: 1185–1193.
8 Miller JD, Hutchins M. The impacts of urbanisation and climate change on urban flooding and urban water quality: A review of the evidence concerning the United Kingdom. *J Hydrol-Regional Studies* 2017; **12**: 345–362.
9 Collet L, Harrigan S, Prudhomme C, *et al.* Future hot-spots for hydro-hazards in Great Britain: A probabilistic assessment. *Hydrol Earth Syst Sci* 2018; **22**: 5387–5401.
10 Visser-Quinn A, Beevers L, Collet L, *et al.* Spatio-temporal analysis of compound hydro-hazard extremes across the UK. *Adv Water Resour* 2019; **130**: 77–90.
11 Kay AL, Rudd AC, Fry M, *et al.* Climate change impacts on peak river flows: Combining national-scale hydrological modelling and probabilistic projections. *Clim Risk Manage* 2021; **31**: 100263.
12 Duan Q, Sorooshian S, Gupta VK. Optimal use of the SCE-UA global optimization method for calibrating watershed models. *J Hydrol* 1994; **158**: 265–284.
13 Gupta HV, Kling H, Yilmaz KK, *et al.* Decomposition of the mean squared error and NSE performance criteria:

Implications for improving hydrological modelling. *J Hydrol* 2009; **377**: 80–91.
14 Gabriel RK, Fan Y. Multivariate hydrologic risk analysis for river thames. *Water* 2022; **14**: 384.
15 Bussi G, Dadson SJ, Prudhomme C, *et al.* Modelling the future impacts of climate and land-use change on suspended sediment transport in the River Thames (UK). *J Hydrol* 2016; **542**: 357–372.
16 Lu Q, Futter MN, Nizzetto L, *et al.* Fate and transport of polychlorinated biphenyls (PCBs) in the River Thames catchment – Insights from a coupled multimedia fate and hydrobiogeochemical transport model. *Sci Total Environ* 2016; **572**: 1461–1470.
17 Bell VA, Kay AL, Cole SJ, *et al.* How might climate change affect river flows across the Thames Basin? An area-wide analysis using the UKCP09 Regional Climate Model ensemble. *J Hydrol* 2012; **442-443**: 89–104.
18 Stevens AJ, Clarke D, Nicholls RJ. Trends in reported flooding in the UK: 1884–2013. *Hydrol Sci J* 2016; **61**: 50–63.
19 Tanguy M, Prudhomme C, Smith K, *et al.* Historic gridded potential evapotranspiration (PET) based on temperature-based equation McGuinness-Bordne calibrated for the UK (1891–2015). NERC Environmental Information Data Centre, 2017. https://doi.org/10.5285/17b9c4f7-1c30-4b6f-b2fe-f7780159939c.
20 Thrasher B, Wang W, Michaelis A, *et al.* NASA global daily downscaled projections, CMIP6. *Sci Data* 2022; **9**: 262.
21 Ziehn T, Chamberlain MA, Law RM, *et al.* The Australian Earth System Model: ACCESS-ESM1.5. *J South Hemisph Earth Syst Sci* 2020; **70**: 193–214.
22 Wu T, Yu R, Lu Y, *et al.* BCC-CSM2-HR: A high-resolution version of the Beijing Climate Center Climate System Model. *Geosci Model Dev* 2021; **14**: 2977–3006.
23 Droogers P, Allen RG. Estimating reference evapotranspiration under inaccurate data conditions. *Irrigation Drainage Syst* 2002; **16**: 33–45.
24 Moore RJ. The probability-distributed principle and runoff production at point and basin scales. *Hydrol Sci J* 1985; **30**: 273–297.
25 Fan YR, Huang GH, Baetz BW, *et al.* Development of integrated approaches for hydrological data assimilation through combination of ensemble Kalman filter and particle filter methods. *J Hydrol* 2017; **550**: 412–426.
26 Moradkhani H, Hsu KL, Gupta H, *et al.* Uncertainty assessment of hydrologic model states and parameters: Sequential data assimilation using the particle filter. *Water Resour Res* 2005; **41**: W05012.
27 Perrin C, Michel C, Andréassian V. Improvement of a parsimonious model for streamflow simulation. *J Hydrol* 2003; **279**: 275–289.
28 Westra S, Thyer M, Leonard M, *et al.* A strategy for diagnosing and interpreting hydrological model nonstationarity. *Water Resour Res* 2014; **50**: 5090–5113.
29 Smith KA, Barker LJ, Tanguy M, *et al.* A multi-objective ensemble approach to hydrological modelling in the UK: An application to historic drought reconstruction. *Hydrol Earth Syst Sci* 2019; **23**: 3247–3268.
30 Jakeman AJ, Hornberger GM. How much complexity is warranted in a rainfall-runoff model? *Water Resour Res* 1993; **29**: 2637–2649.
31 Jakeman AJ, Littlewood IG, Whitehead PG. Computation of the instantaneous unit hydrograph and identifiable component flows with application to two small upland catchments. *J Hydrol* 1990; **117**: 275–300.
32 Vaze J, Post DA, Chiew FHS, *et al.* Climate non-stationarity – Validity of calibrated rainfall-runoff models for use in climate change studies. *J Hydrol* 2010; **394**: 447–457.
33 Viney NR, Bormann H, Breuer L, *et al.* Assessing the impact of land use change on hydrology by ensemble modelling (LUCHEM) II: Ensemble combinations and predictions. *Adv Water Resour* 2009; **32**: 147–158.
34 Shin MJ, Guillaume JHA, Croke BFW, *et al.* Addressing ten questions about conceptual rainfall-runoff models with global sensitivity analyses in R. *J Hydrol* 2013; **503**: 135–152.
35 Shin MJ, Guillaume JHA, Croke BFW, *et al.* A review of foundational methods for checking the structural identifiability of models: Results for rainfall-runoff. *J Hydrol* 2015; **520**: 1–16.
36 Shin MJ, Kim CS. Assessment of the suitability of rainfall-runoff models by coupling performance statistics and sensitivity analysis. *Hydrol Res* 2017; **48**: 1192–1213.

37 Croke B, Jakeman A. Use of the IHACRES rainfall-runoff model in arid and semi-arid regions. In: Wheater H, Sorooshian S, Sharma K (Eds.). *Hydrological Modelling in Arid and Semi-Arid Areas (International Hydrology Series)*. Cambridge: Cambridge University Press, 2007, 41–48.

38 Fan YR, Shi X, Duan QY, *et al.* Towards reliable uncertainty quantification for hydrologic predictions. Part I: Development of a particle copula Metropolis Hastings method. *J Hydrol* 2022; **612**: 128163.

39 Fan YR, Shi X, Duan QY, *et al.* Towards reliable uncertainty quantification for hydrologic predictions. Part II: Characterizing impacts of uncertain factors through an iterative factorial data assimilation framework. *J Hydrol* 2022; **612**: 128136.

40 Duan Q, Pappenberger F, Wood A, *et al. Handbook of Hydrometeorological Ensemble Forecasting*. Berlin, Heidelberg: Springer, 2019.

41 Liu Z, Cheng L, Lin K, *et al.* A hybrid bayesian vine model for water level prediction. *Environ Model Software* 2021; **142**: 105075.

42 Raftery AE, Gneiting T, Balabdaoui F, *et al.* Using bayesian model averaging to calibrate forecast ensembles. *Mon Weather Rev* 2005; **133**: 1155–1174.

43 Wu H, Su X, Singh VP, *et al.* Bayesian vine copulas improve agricultural drought prediction for long lead times. *Agric For Meteor* 2023; **331**: 109326.

44 Yang T, Liu X, Wang L, *et al.* Simulating hydropower discharge using multiple decision tree methods and a dynamical model merging technique. *J Water Resour Plann Manage* 2020; **146**: 04019072.

45 Yang T, Tao Y, Li J, *et al.* Multi-criterion model ensemble of CMIP5 surface air temperature over China. *Theor Appl Climatol* 2018; **132**: 1057–1072.

46 Duan Q, Ajami NK, Gao X, *et al.* Multi-model ensemble hydrologic prediction using Bayesian model averaging. *Adv Water Resour* 2007; **30**: 1371–1386.